

# Journal of Materials Chemistry B

Accepted Manuscript



This article can be cited before page numbers have been issued, to do this please use: Y. Zhang, L. Ma, C. Tang, S. Pan, D. Shi, S. Wang, M. Li and Y. Guo, *J. Mater. Chem. B*, 2018, DOI: 10.1039/C7TB02862H.



This is an Accepted Manuscript, which has been through the Royal Society of Chemistry peer review process and has been accepted for publication.

Accepted Manuscripts are published online shortly after acceptance, before technical editing, formatting and proof reading. Using this free service, authors can make their results available to the community, in citable form, before we publish the edited article. We will replace this Accepted Manuscript with the edited and formatted Advance Article as soon as it is available.

You can find more information about Accepted Manuscripts in the [author guidelines](#).

Please note that technical editing may introduce minor changes to the text and/or graphics, which may alter content. The journal's standard [Terms & Conditions](#) and the ethical guidelines, outlined in our [author and reviewer resource centre](#), still apply. In no event shall the Royal Society of Chemistry be held responsible for any errors or omissions in this Accepted Manuscript or any consequences arising from the use of any information it contains.



Journal Name

ARTICLE

## A highly sensitive and rapidly responding fluorescent probe based on a rhodol fluorophore for imaging endogenous hypochlorite in living mice

Yanhui Zhang<sup>a</sup>, Lin Ma<sup>b</sup>, Chunchao Tang<sup>b</sup>, Shengnan Pan<sup>a</sup>, Donglei Shi<sup>a</sup>, Shaojing Wang<sup>a</sup>, Minyong Li<sup>b,\*</sup> and Yuan Guo<sup>a,\*</sup>

Received 00th January 20xx,  
Accepted 00th January 20xx

DOI: 10.1039/x0xx00000x

www.rsc.org/

Hypochlorous (HOCl) acid is generated as a defense tool in the immune system and plays a vital role in killing a wide range of pathogens. There is therefore great interest in developing fluorescent probes that can endogenously respond to the change in concentration of HOCl *in vivo*. To address this challenge, we here present a rapidly responding fluorescent probe **RO610** to image endogenous HOCl in living mice. The development of **RO610** was based on a novel water-soluble and pH-independent fluorescent xanthene dye, 2'-formylrhodol **ROA**, which exhibits highly selective and sensitive responses to HOCl/CIO<sup>-</sup> over other reactive species. Moreover, adding a little more than 5 equiv. of CIO<sup>-</sup> to the solution of **RO610** resulted in a clearly observable fluorescence enhancement (48-fold) within 30 s. Based on these properties, **RO610** was used to detect CIO<sup>-</sup> in A549 cells without interference by other oxidants. It was applied for the imaging of endogenous HOCl in living nude mice with satisfactory results.

### Introduction

Hypochlorous acid (HOCl)/hypochlorite (CIO<sup>-</sup>) is known to be one of the biologically important reactive oxygen species (ROS).<sup>1</sup> It is widely employed in our daily life as a bleaching agent and a disinfectant for potable water.<sup>2</sup> Biologically, the generation of endogenous hypochlorite is driven by hydrogen peroxide and chloride ions in activated neutrophils catalyzed by a heme-containing enzyme myeloperoxidase (MPO).<sup>3</sup> Nevertheless, abnormal levels of hypochlorite can contribute to tissue damage and diseases such as nephropathy, atherosclerosis, cardiovascular disease and cancers.<sup>4</sup> In order to comprehend the vital role hypochlorite plays in the biosystem, it is important to develop techniques for real-time monitoring and accurate detection of CIO<sup>-</sup>. In particular, fluorescent probes have become a powerful tool for sensing trace amounts of species in chemical and biological samples due to the high sensitivity, specificity, simplicity of implementation and fast response of fluorescence detection.<sup>5</sup> Unfortunately, the feasibility of using fluorescence methods for a particular application is often limited by

the availability of appropriate fluorescent molecules. Although a number of fluorescent probes have been reported based on traditional fluorophores, some drawbacks can be encountered, such as single emission intensity, low quantum yield and short emission wavelength.<sup>6</sup> There is therefore a growing need to develop a fluorescent probe which is able to overcome these limitations based on novel and efficient fluorophores. In recent years, with the hybrid structure of fluorescein and rhodamine, rhodol fluorophores and derivatives thereof (also named "Rhodafluor")<sup>7,8</sup> have been found to be excellent and interesting candidates for fluorescent probes since they inherit all the superior photophysical properties from fluorescein and rhodamine, such as high extinction coefficients, quantum yield, photostability and solubility in a variety of solvents. Based on the relationships between the structures of rhodol derivatives and their excellent photophysical and photochemical properties, we presumed that the reasonable modification of the xanthene skeleton of rhodol would allow us to optimize the photophysical properties of rhodol dyes for the desired applications. Herein, we present a new rhodol dye, **ROA** (2'-formylrhodol), which readily dissolves in water in the form of a ring-opened zwitterion structure. Moreover, it has high quantum yields ( $\Phi = 0.94$ , measured in ethanol) and displays strong tolerance to pH, being capable of generating stable optical signals in the pH range of 5.5-9. More interestingly, colorimetric and ratiometric sensing systems can be established by modifying or using directly the active formyl, carboxyl and hydroxyl of **ROA**.

We also developed a novel "turn-on" fluorescence probe **RO610** via the condensation reaction between the formyl group of **ROA** as a fluorophore and diaminomaleonitrile. It is known

<sup>a</sup> Key Laboratory of Synthetic and Natural Functional Molecule Chemistry of the Ministry of Education, College of Chemistry and Materials Science, Northwest University, 1 Xuefu Ave, P. R. China. \*Email: guoyuan@nwu.edu.cn

<sup>b</sup> Department of Medicinal Chemistry, Key Laboratory of Chemical Biology (MOE), School of Pharmacy, Shandong University, Jinan, Shandong 250012, China. \*E-mail: mli@sdu.edu.cn

†Electronic Supplementary Information (ESI) available: Chemical structures, Supplementary spectra, NMR and HRMS data, cell viability assays. See DOI: 10.1039/x0xx00000x

that C=N isomerization is the predominant decay process of excited states in compounds with an unfixed C=N structure.<sup>9</sup> Thus, as expected, **RO610** itself was nearly non-fluorescent due to C=N isomerization, while the strong yellow fluorescence was restored upon addition of ClO<sup>-</sup>. The phenomenon occurred by the formation of a formyl group which was caused by oxidation and hydrolysis of C=N. Most notably, the fluorescence-on reaction showed high sensitivity (LOD, 2.88 × 10<sup>-8</sup> M), high selectivity and a rapid response time (30 s) for ClO<sup>-</sup> over other common oxidants and nucleophiles, which makes it practical for detecting ClO<sup>-</sup> in cells and mice.

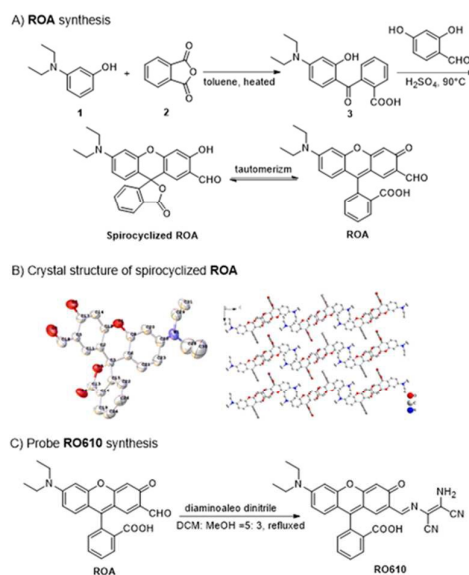


**Fig. 1** (A) Synthetic route of the **ROA**. (B) The crystal structure of spirocyclized **ROA**. (C) Synthesis of the probe **RO610**.

## Materials and methods

### Materials and instruments

Unless otherwise specified, all materials were obtained from commercial suppliers and used without further purification. All inorganic salts used were of analytical grade. Twice-distilled water was used throughout the experiments. A Mettler Toledo pH meter was used to determine the pH. <sup>1</sup>H NMR and <sup>13</sup>C NMR spectra were recorded on a VARIAN INOVA-400 spectrometer, using TMS as an internal standard. Mass spectrometry data were obtained with an AXIMA-CFR plus MALDI-TOF Mass Spectrophotometer. UV-visible spectra were collected on a Shimadzu U-1700 spectrophotometer. Fluorescence measurements were performed on a Hitachi F-4500 fluorescence spectrophotometer with a xenon discharge lamp, in a 1 cm quartz cell. HPLC spectra were collected on an Agilent HP1100 high performance liquid chromatograph. The ability of probes reacting to hypochlorite in the cells was also evaluated by laser confocal fluorescence imaging using an Olympus FV1000 laser scanning microscope.

### General UV-vis and fluorescence spectra measurements

A stock solution of **RO610** (1.0 mM) was prepared in acetone. Stock solutions (10 mM) of various analytes were prepared by dissolving an appropriate amount of the test species in water. Various ROS and RNS including ClO<sup>-</sup>, H<sub>2</sub>O<sub>2</sub>, <sup>•</sup>OH, <sup>1</sup>O<sub>2</sub>, O<sub>2</sub><sup>•-</sup>, NO<sup>•</sup>, *t*-BuOOH and TBO<sup>•</sup> were prepared according to previous reports.<sup>11</sup> All UV-vis and fluorescence titration experiments were performed for 5 min at room temperature using EtOH/phosphate buffer (20 mM, pH 7.4, 3:7) solution. Any changes in the fluorescence intensity were monitored using a fluorescence spectrometer (λ<sub>ex</sub> = 535 nm, λ<sub>em</sub> = 577 nm, slit: 5 nm/5 nm).

### Measurement of fluorescence quantum yields

The fluorescence quantum yields were determined using Rhodamine B as a reference with a known Φ value of 0.89 in EtOH.<sup>12</sup> The sample and the reference were excited at the same wavelength (λ<sub>ex</sub> = 495 nm), maintaining nearly equal absorbance (0.05). The quantum yield was estimated following the equation (1):

$$\Phi_S/\Phi_R = (A_S/A_R) \times (Abs_R/Abs_S) \times (\eta_S^2/\eta_R^2) \quad (1)$$

where Φ<sub>S</sub> and Φ<sub>R</sub> are the fluorescence quantum yields of the sample and the reference, respectively; A<sub>S</sub> and A<sub>R</sub> are the emission areas of the sample and the reference, respectively; Abs<sub>S</sub> and Abs<sub>R</sub> are the corresponding absorbances of the sample and the reference solution at the excitation wavelength of excitation; η<sub>S</sub> and η<sub>R</sub> are the refractive indices of the sample and the reference, respectively.

### Cytotoxicity assay

The methyl thiazolyl tetrazolium (MTT) assay with A549 was used to identify the cytotoxic potential of **RO610**. 90% confluence A549 cells were seeded into a 96-well cell-culture plate with density of 5000 cells per hole. After incubating for 24 h, different concentrations of **RO610** (5, 10, 15, 20, 25, 30 μM) were added to the wells. The cells were treated and incubated at 37 °C under 5% CO<sub>2</sub> for another 24 h. 10 μL MTT was added to each well and incubated for 4 h in the same conditions. The MTT solution was removed and yellow precipitates (formazan) observed in the plates were dissolved in 200 μL DMSO. The absorbance was recorded at 490 nm using the microplate spectrophotometer system (Varioskan Flash). The viability of the cells was calculated by the ratio of mean of the absorbance value of the treatment group and the control group.

### Animals

All animal studies were approved by the Ethics Committee and IACUC of Qilu Health Science Center, Shandong University, and were conducted in compliance with European guidelines for the care and use of laboratory animals. Imaging procedures were conducted with adult mice (4-6 weeks old, 15-18 g, Shandong University, Jinan, China) under general anesthesia by injection of sodium pentobarbital (0.5 ml/0.03%).

## Results and discussion

### Synthesis and characterization

**Synthesis of Compound 3.** 1.00 g (6.05 mmol) 3-diethylaminophenol and 1.07 g (7.26 mmol) *o*-phthalic anhydride were gradient heated in 15 mL methylbenzene for 10 h, 80 °C; 5 h, 90 °C; 2 h, 100 °C; 1 h, 110 °C. Then, the reaction mixture was refluxed for 1 h. After the reaction was complete, the mixture solution was cooled then filtered and washed with methanol. The pink solid thus obtained was dried to give compound **3** in 25% yield. <sup>1</sup>H NMR (400 MHz, DMSO-*d*<sub>6</sub>): δ ppm 13.11 (s, 1H), 12.59 (s, 1H), 7.97 (d, J = 7.2 Hz, 1H), 7.68 (t, J = 7.2 Hz, 1H), 7.60 (t, J = 7.4 Hz, 1H), 7.37 (d, J = 7.2 Hz, 1H), 6.80-6.78 (m, 1H), 6.17 (d, J = 9.2 Hz, 1H), 6.08 (s, 1H), 3.37 (q, J = 6.4 Hz, 4H), 1.08 (t, J = 6.2 Hz, 6H).

**Synthesis of Compound ROA.** A mixture of 300 mg (0.96 mmol) **3** and 132 mg (0.96 mmol) 2,4-dihydroxybenzaldehyde was added in 5 mL of sulfuric acid and stirred at 90 °C monitoring with TLC. After the reaction was complete, the mixture solution was cooled to room temperature and then poured into ice-cold water (100 mL). After adjusting the pH value of the mixture to 7-8 with ammonium hydroxide, the precipitate was filtered, washed with brine, and then dried under vacuum to give the crude product, which was further purified by chromatography on a silica gel column (CH<sub>2</sub>Cl<sub>2</sub>:CH<sub>3</sub>OH = 300:1 v:v) to give a red product **ROA** in 30% yield. <sup>1</sup>H NMR (400 MHz, CDCl<sub>3</sub>): δ ppm 11.19 (s, 1H), 9.57 (s, 1H), 8.05 (d, J = 7.2 Hz, 1H), 7.68 (m, 2H), 7.22 (d, J = 7.6 Hz, 1H), 7.01 (s, 1H), 6.80 (s, 1H), 6.57 (d, J = 8.8 Hz, 1H), 6.48 (s, 1H), 6.39 (d, J = 8.4 Hz, 1H), 3.37 (q, J = 6.8 Hz, 4H), 1.18 (t, J = 6.8 Hz, 6H); <sup>13</sup>C NMR (100 MHz, CDCl<sub>3</sub>): 194.62, 169.28, 162.91, 157.83, 152.47, 152.19, 149.71, 135.49, 135.07, 129.83, 128.72, 126.94, 125.92, 125.07, 123.86, 117.80, 113.24, 108.86, 104.45, 104.37, 97.67, 82.99, 44.45, 12.38; ESI-HRMS: [M+H]<sup>+</sup> m/z 416.1483, calcd for C<sub>25</sub>H<sub>22</sub>NO<sub>5</sub> 416.1492; FT-IR ν (KBr, cm<sup>-1</sup>): 3672.28, 1750.47, 1625.98, 1521.23, 1405.66, 875.84, 801.42, 697.41.

**Synthesis of the Probe RO610.** To a suspended solution of compound **ROA** (83.05 mg, 0.2 mmol) in CH<sub>3</sub>OH:CH<sub>2</sub>Cl<sub>2</sub> = 5:3 (4 mL) was added an excess of 2,3-diamino-2-butenedinitrile (32.43 mg, 0.3 mmol) and the solution was refluxed and monitored with TLC. After the reaction was complete, the mixture solution was cooled to room temperature. The yellow solid formed was filtered and washed with a small amount of methanol several times. 64.67 mg brown probe **RO610** was dried in vacuum and then obtained with a yield of 64%. <sup>1</sup>H NMR (400 MHz, Acetone-*d*<sub>6</sub>): δ ppm 8.46 (s, 1H), 7.97 (d, J = 7.2 Hz, 1H), 7.80 (t, J = 7.2 Hz, 1H), 7.73 (t, J = 7.6 Hz, 1H), 7.39 (s, 1H), 7.33 (d, J = 7.6 Hz, 1H), 7.13 (s, 2H), 6.79 (s, 1H), 6.57 (d, J = 9.6 Hz, 1H), 6.52-6.51 (m, 2H), 3.44 (q, J = 6.8 Hz, 4H), 1.17 (t, J = 6.8 Hz, 6H); <sup>13</sup>C NMR (100 MHz, Acetone-*d*<sub>6</sub>): δ 210.57, 173.79, 166.24, 164.64, 160.69, 157.79, 157.61, 154.96, 140.30, 139.57, 135.06, 133.98, 132.50, 130.39, 129.78, 129.24, 121.78, 119.14, 118.43, 117.93, 114.16, 110.55, 109.77, 108.52, 102.56, 49.30, 17.07; HRMS (ESI): [M+H]<sup>+</sup> m/z 506.1831, calcd for C<sub>29</sub>H<sub>24</sub>N<sub>5</sub>O<sub>4</sub> 506.1823; FT-IR ν (KBr, cm<sup>-1</sup>): 3432, 2976, 2233, 2205, 1739, 1626, 1501, 1373, 1264, 1215, 1108, 874, 767, 692, 546.

### Optical properties of ROA

Firstly, the photochemical properties of **ROA** in solvents with different polarities were investigated by fluorescence measurements (Fig. 2a). In polar solvent, the **ROA** was ring-opened and exhibited a strong fluorescence intensity at 577nm, which was attributed to the π-π\* transitions of the ring-opened xanthene conjugate. In order to verify the fluorescence mechanism further, the fluorescence features were investigated by TD-DFT calculations. Based on the optimized geometry of **ROA**, it was found that the strongest fluorescence peak came from the HOMO-LUMO transition, and partly from the HOMO-1-LUMO transition. The three orbitals (HOMO-1, HOMO and LUMO) are π type distributed on the conjugate plane of **ROA** (shown in Fig. S10), corresponding to the π-π\* transition rather than to ICT between diethylin and formyl groups. In contrast, **ROA** was spirocyclized without any fluorescence in aprotic solvent. These results indicated that **ROA** is sensitive to the solvent. Furthermore, we obtained the crystal structure of spirocyclized **ROA** (CCDC number: 1588170, Fig. 1, Fig. S3 and Table S1) by slowly evaporating its dichloromethane solution at room temperature which also proved that the spiro lactone structure of **ROA** is stable in the most aprotic organic solvents. Conversely, it showed a ring-opened π-conjugate form in the protic solvent resulting in strong fluorescent emission. Therefore, the compound **ROA** can be easily modified by chemical approaches because of its various modifiable sites of interconversion structures in different solvents, which is of paramount importance for the molecular design of the compound as a signaling fluorophore for chemosensors and biological applications (Fig. S1). A continuous pH titration of **ROA** in water revealed that there was enhanced emission at 577 nm from pH 1.5 to 12 (Fig. 2b). We also found that the response to changes in pH fitted a sigmoid curve in a pH range of 2-6 and 9-11.5 (see Fig. S2a). The pK<sub>a</sub> of 4.54 and 11.5 were calculated by using the Henderson-Hasselbach-type mass action equation (see Fig. S2b). Interestingly, ring-opened **ROA** showed a stable fluorescence signal from pH 5.5 to 9, implying that the pH independent properties meet the requirements of fluorescent labels or tracers for biological applications.

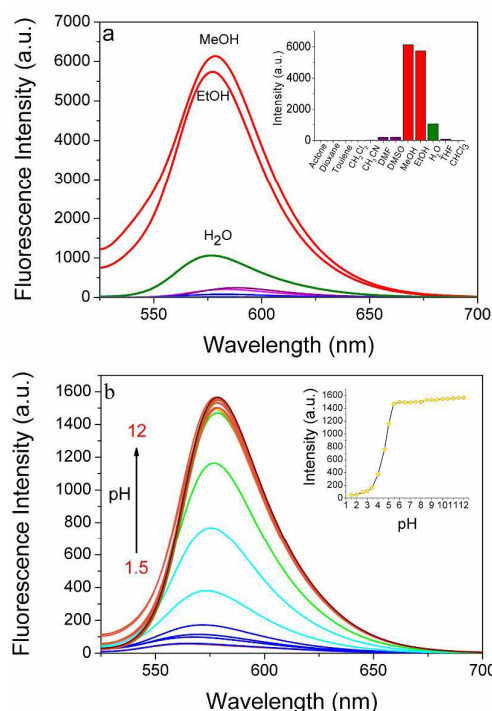


**Fig. 2** (a) Emission spectra of **ROA** (10  $\mu\text{M}$ ) in different solvents. (b) in different pH solutions. Inset: Fluorescent intensity of **ROA** at 577 nm under different pH conditions. ( $\lambda_{\text{ex}} = 515 \text{ nm}$ ,  $\lambda_{\text{em}} = 577 \text{ nm}$ , slit: 5 nm/5 nm).

#### Kinetic studies of **RO610** towards $\text{ClO}^-$ and titration experiments

To test the sensing ability of the probe **RO610** for  $\text{ClO}^-$ , we studied its optical spectrum in phosphate buffer:EtOH = 7: 3 (V/V, 20 mM, pH = 7.4) at room temperature (25  $^{\circ}\text{C}$ ). Fig. 3a shows the response time chart for the chemosensor upon contact with  $\text{ClO}^-$  under these conditions. The data indicate that the fluorescent intensity increased dramatically in 30 s and then leveled off, while the fluorescence background of the detection system in the absence of  $\text{ClO}^-$  remained unchanged at the same time. To obtain a high sensitivity and reproducible results, a 5 min reaction time was selected in the following experiment.

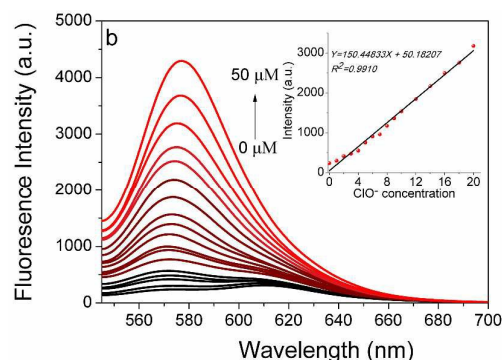
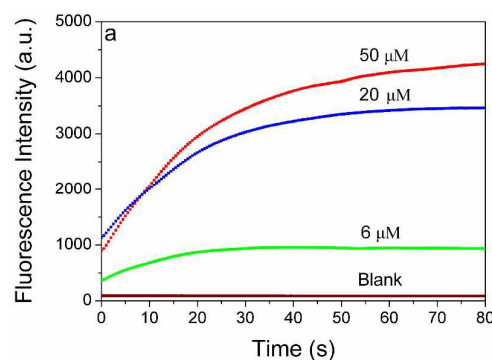


**Fig. 3** (a) Kinetic analysis of **RO610** towards  $\text{ClO}^-$  (0, 6, 20, 50  $\mu\text{M}$ ). (b) Fluorescence emission spectra of **RO610** (10  $\mu\text{M}$ ) upon the addition of increasing concentrations of sodium hypochlorite (0–50  $\mu\text{M}$ ). Inset: linear plot of emission changes at 577 nm against  $\text{ClO}^-$  concentration ( $\lambda_{\text{ex}} = 535 \text{ nm}$ ,  $\lambda_{\text{em}} = 577 \text{ nm}$ , slit: 5 nm/5 nm).

We then implemented the titration experiments with addition of  $\text{ClO}^-$  in the **RO610** solution (10  $\mu\text{M}$ ) to evaluate the quantitative detection capacity and detection limit. As shown in Fig. 3b, **RO610** displays weak fluorescence (fluorescence quantum yield  $\Phi = 0.04$ ). When  $\text{ClO}^-$  was titrated from 0 to 50  $\mu\text{M}$ , the mixture of **RO610** exhibited a 48-fold enhancement of fluorescence intensity over that of blank (fluorescence quantum yield  $\Phi = 0.35$ ), and the phenomenon of brightness enhancement could be observed by the naked eye under a 365 nm UV lamp. This can be attributed to the formation of **ROA** by the reaction of **RO610** with  $\text{ClO}^-$ , which was confirmed by  $^1\text{H}$  NMR and HRMS. Additionally, the UV-vis spectra of **RO610** exhibited maximum absorption at 572 nm. Upon addition of  $\text{ClO}^-$ , the absorption at 572 nm decreased, whereas a new absorption peak appeared at 542 nm which changed the color of the solution from purple to pink, indicating the colorimetric detection of  $\text{ClO}^-$  (Fig. S4). The absorption and emission spectra showed that the changes reached a plateau when the concentration of  $\text{ClO}^-$  increased to 50  $\mu\text{M}$ . What is more, the fluorescence intensity of **RO610** has a good linear relationship with the  $\text{ClO}^-$  concentration ranging from 0 to 20  $\mu\text{M}$ , suggesting that the probe is potentially useful for quantitatively detecting  $\text{ClO}^-$ . Accordingly, the detection limit ( $3\sigma/\text{slope}$ ) was as low as  $2.88 \times 10^{-8} \text{ M}$ .

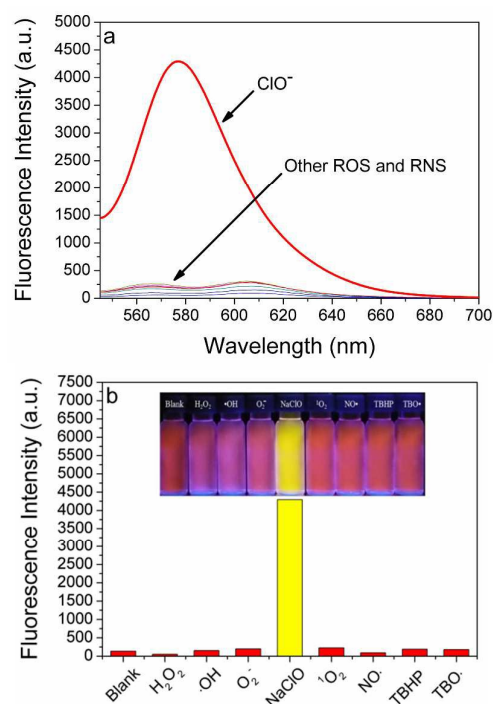


**Fig. 4** (a) Fluorescence spectra of probe **RO610** (10  $\mu\text{M}$ ) in the presence of 200  $\mu\text{M}$  analytes ( $\text{H}_2\text{O}_2$ ,  $\cdot\text{OH}$ ,  $\text{O}_2^{\cdot-}$ ,  $^1\text{O}_2$ ,  $\text{NO}\cdot$ , TBHP,  $\text{TBO}\cdot$ ) and 50  $\mu\text{M}$   $\text{ClO}^-$ . (b) Optical density graph of the emission at 577 nm of probe **RO610** (10  $\mu\text{M}$ ) upon the addition of several analytes for 5 min and inset: visual fluorescence color (under a handheld 365 nm UV lamp) changes. ( $\lambda_{\text{ex}} = 535 \text{ nm}$ ,  $\lambda_{\text{em}} = 577 \text{ nm}$ , slit: 5 nm/5 nm).

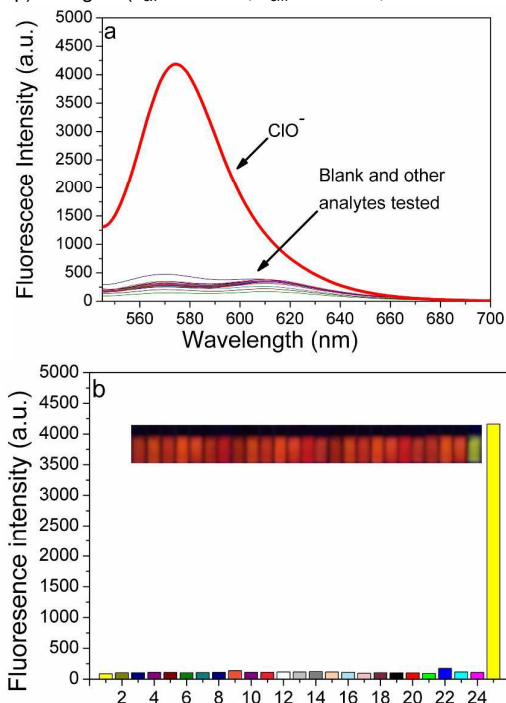


**Fig. 5** (a) Fluorescence spectra of probe **RO610** (10  $\mu\text{M}$ ) in phosphate buffer : EtOH = 7 : 3 (V/V, 20 mM, pH = 7.4) in the presence of 200  $\mu\text{M}$  of various analytes; (b) Optical density graph of the emission at 577 nm of

probe **RO610** (10  $\mu\text{M}$ ) upon the addition of several analytes and inset: visual fluorescence color (under a handheld 365 nm UV lamp) changes (1: Blank; 2:  $\text{F}^-$ ; 3:  $\text{Cl}^-$ ; 4:  $\text{Br}^-$ ; 5:  $\text{I}^-$ ; 6:  $\text{S}_2\text{O}_3^{2-}$ ; 7:  $\text{AcO}^-$ ; 8:  $\text{SO}_4^{2-}$ ; 9:  $\text{NO}_2^-$ ; 10:  $\text{NO}_3^-$ ; 11:  $\text{CN}^-$ ; 12:  $\text{HS}^-$ ; 13:  $\text{SCN}^-$ ; 14:  $\text{PO}_4^{3-}$ ; 15:  $\text{H}_2\text{PO}_4^-$ ; 16:  $\text{HPO}_4^{2-}$ ; 17:  $\text{CO}_3^{2-}$ ; 18:  $\text{HCO}_3^-$ ; 19:  $\text{HSO}_4^-$ ; 20:  $\text{HSO}_3^-$ ; 21:  $\text{SO}_3^{2-}$ ; 22: Cys; 23: Hcy; 24: GSH; 25:  $\text{ClO}^-$ ) ( $\lambda_{\text{ex}} = 535 \text{ nm}$ ,  $\lambda_{\text{em}} = 577 \text{ nm}$ , slit: 5 nm/5 nm).

#### Selectivity of **RO610** towards $\text{ClO}^-$

As achieving a high selectivity toward the target molecule is a major issue in the field of molecular sensing, we tested the sensing performance of the probe **RO610** towards various reactive oxygen species (ROS) and reactive nitrogen species (RNS), including sodium hypochlorite ( $\text{NaOCl}$ ), hydrogen peroxide ( $\text{H}_2\text{O}_2$ ), hydroxyl radicals ( $\cdot\text{OH}$ ), superoxide ( $\text{O}_2^{\cdot-}$ ), singlet oxygen ( $^1\text{O}_2$ ), nitric oxide ( $\text{NO}\cdot$ ), *tert*-butyl hydroperoxide (TBHP) and *tert*-butoxy radical ( $\text{TBO}\cdot$ ) in a phosphate buffer solution. Strong yellow fluorescence was only observed upon the addition of  $\text{ClO}^-$  to a solution containing **RO610**; the other ROS and RNS produced no obvious change in fluorescence (Fig. 4). The same result was obtained by the UV-vis spectrum (Fig. S6). Considering that the nucleophilic addition of common anions and biothiols might act on the position of the dicyanovinyl groups present in the chemosensor and thus break the conjugation, which ultimately offsets the effect of C=N isomerization and leads to fluorescence enhancement, the fluorescent response of **RO610** towards various common anions and biothiols was explored (Fig. 5). When 200  $\mu\text{M}$  anions ( $\text{F}^-$ ,  $\text{Cl}^-$ ,  $\text{Br}^-$ ,  $\text{I}^-$ ,  $\text{S}_2\text{O}_3^{2-}$ ,  $\text{AcO}^-$ ,  $\text{SO}_4^{2-}$ ,  $\text{NO}_2^-$ ,  $\text{NO}_3^-$ ,  $\text{CN}^-$ ,  $\text{HS}^-$ ,  $\text{SCN}^-$ ,  $\text{PO}_4^{3-}$ ,  $\text{H}_2\text{PO}_4^-$ ,  $\text{HPO}_4^{2-}$ ,  $\text{CO}_3^{2-}$ ,  $\text{HCO}_3^-$ ,  $\text{HSO}_4^-$ ,  $\text{HSO}_3^-$ ,  $\text{SO}_3^{2-}$ ) and 200  $\mu\text{M}$  biothiols (Cys, Hcy, GSH) were added to 10  $\mu\text{M}$  **RO610** in phosphate buffer, none of the ions produced a noticeable change in the fluorescence intensity, indicating no response toward the **RO610** probe. Moreover, other analytes showed negligible changes in absorbance spectra under the same conditions. Thus, these results suggest that **RO610** possesses a higher selectivity for  $\text{ClO}^-$  and a potential application for detecting  $\text{ClO}^-$  in complex biological environments.

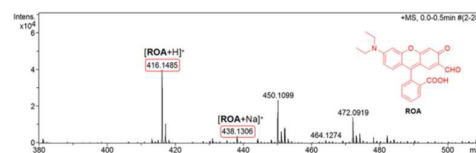
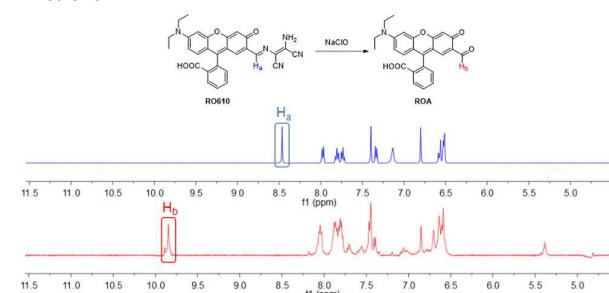


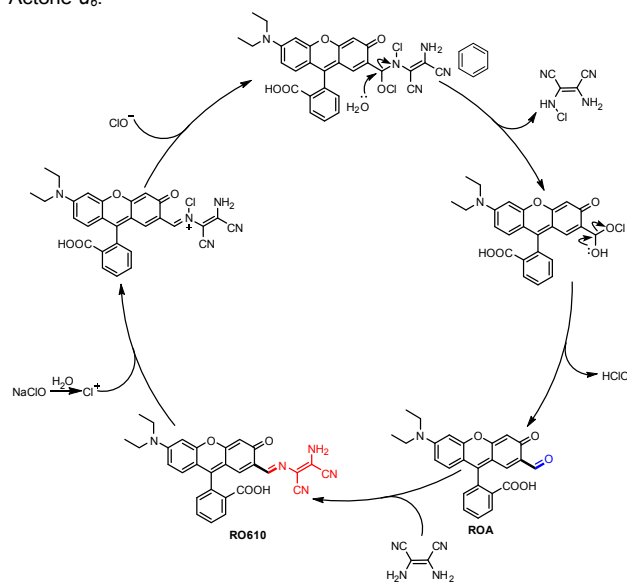
**Fig. 6** ESI-MS spectra of mixture of **RO610** (10  $\mu\text{M}$ ) with 5 equiv. of  $\text{NaOCl}$  in methanol.



## ARTICLE

## Journal Name

**Fig. 7**  $^1\text{H}$  NMR spectrum of probe **RO610** and the product of the complete reaction mixture of the probe **RO610** with 5 equiv.  $\text{ClO}^-$  in Acetone- $d_6$ .



**Scheme 1** The proposed recognition mechanism of **RO610** towards hypochlorite.

### The proposed $\text{ClO}^-$ sensing mechanism of **RO610**

In order to investigate the mechanism of the reaction of probe **RO610** with  $\text{ClO}^-$ , a series of experiments was performed. The proposed mechanism is shown in Scheme 1. According to the coincident peak at normalized emission and absorbance spectra (Fig. S7), we assumed that the product of this probe oxidized by  $\text{ClO}^-$  was **ROA**, which was confirmed by the ESI-MS spectra of the reaction mixture of the probe with 5 equiv.  $\text{ClO}^-$ . The ESI-MS showed the presence of a dominant peak at  $m/z = 416.1485$ , which corresponded to **ROA** ( $m/z = 416.1492$  [ $\text{ROA}+\text{H}]^+$ ) (Fig. 6).  $^1\text{H}$  NMR spectra also confirmed the hypochlorite mediated conversion of **RO610** to **ROA**. The  $^1\text{H}$  NMR titrating experiment revealed that the presence of  $\text{ClO}^-$  in the **RO610** solution caused the disappearance of the signal at 8.46 ppm ( $-\text{CH}=\text{N}$  proton of **RO610**) and the appearance of a new signal at 9.85 ppm ( $-\text{CHO}$  proton of **ROA**) (Fig. 7). However, as shown in Fig. 7, the attribution of some peaks could not be specified. We suspected that there could be by-products generated, combined with the above result of no clear isosbestic point in the UV-vis spectrum (Fig. S4). An HPLC experiment was therefore carried out to confirm the conversion yield of **ROA**. The results showed that **ROA** was still the main product and that the yield of **ROA** calculated by the normalization method was 89% (Fig. S11).

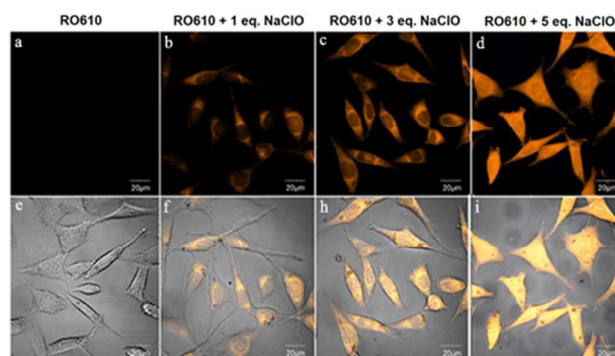


**Fig. 8** Confocal fluorescence images of A549 cells. Fluorescence image (a-d) and merge (e-i) of A549 cells pretreated with 5  $\mu\text{M}$  probe **RO610** for 10 min and then followed by incubation with 0, 5, 15, 25  $\mu\text{M}$  of  $\text{ClO}^-$  for 10 min, respectively. The cells were excited with a light laser at 543 nm, and emission was collected at 555–655 nm. Scale bar: 20  $\mu\text{m}$ .

### Bioimaging and cytotoxicity studies

Encouraged by the desirable optical response in aqueous solution, we then explored the capability of **RO610** to monitor  $\text{ClO}^-$  in a cellular context using confocal fluorescence imaging. Prior to that, an MTT assay was conducted to evaluate the cytotoxicity of **RO610**. The cellular viability was estimated to be greater than 80% after 24 h, indicating that the probe (<30  $\mu\text{M}$ ) has low cytotoxicity (Fig. S8). The A549 cells incubated with only **RO610** (5  $\mu\text{M}$ , 10 min) displayed very dim fluorescence (Fig. 8). However, after the treatment with 5  $\mu\text{M}$ , 15  $\mu\text{M}$  and 25  $\mu\text{M}$   $\text{ClO}^-$ , a significant enhancement of the fluorescence was observed in the yellow channel and it was clearly seen that the fluorescence intensities of the cells rose along with an increase in  $\text{ClO}^-$  concentration. These data indicate that probe **RO610** is cell membrane permeable and capable of imaging of  $\text{ClO}^-$  in cells.

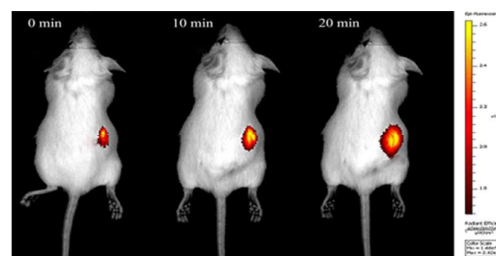


**Fig. 9** Representative fluorescence images (pseudocolor) of a mouse given a skin-pop injection of **RO610** (25  $\mu\text{L}$ , 1 mM, right abdomen) and a subsequent (10 min later) skin-pop injection of  $\text{ClO}^-$  (5.0 equiv.) in the same region. Images were taken after incubation for 0, 10 and 20 min, respectively. Images were taken using an excitation laser at 530 nm and a 600 nm emission filter.

The suitability of the probe for visualizing  $\text{ClO}^-$  in living was also evaluated. All these images were obtained from normal mice without unhairing. The mouse was given an s.p. (skin-pop) injection of **RO610** (1 mM, 25  $\mu\text{L}$  DMSO) on the right abdomen, and 10 minutes later, the mouse was given an

s.p. injection of 5.0 equiv. of  $\text{ClO}^-$  in the same region. The mouse was imaged by using an IVIS Spectrum small animal in vivo imaging system with a 530 nm excitation laser and a 600 nm emission filter. Fig. 9 shows representative fluorescence images of a mouse at different times after the injection of  $\text{ClO}^-$ . It was demonstrated that the fluorescence intensity was enhanced gradually within 20 min, proving that **RO610** can detect  $\text{ClO}^-$  in vivo without the interference of background signals.

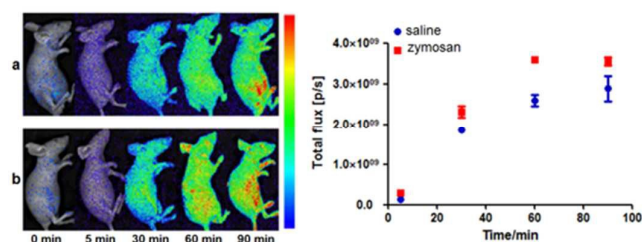


**Fig. 10** (Left) Representative fluorescence images of a nude mouse. a, The mouse was given an intraperitoneal injection of saline (1 mL) for 5 h, finally a intraperitoneal injection of **RO610** (0.2 mL, 1 mM). b, The mouse was given an intraperitoneal injection of zymosan (1 mL, 1 mg/mL) for 5 h, subsequent an intraperitoneal injection of **RO610** (0.2 mL, 1 mM). Images were taken after incubation for 0, 5, 10, 30, 60 and 90 min, respectively. (Right) Fluorescence intensities of nude mouse in panels a, b. Images were taken using an excitation laser of 535 nm and an emission filter of 570 nm.

Subsequently, we explored the feasibility of detecting endogenous  $\text{ClO}^-$  in vivo. According to the literature,<sup>13</sup> zymosan can stimulate cells to produce  $\text{ClO}^-$ . As shown in Fig. 10, The fluorescence measured at the abdomen increased markedly after zymosan injection, and strong fluorescence was observed at 90 min. Interestingly, control, unstimulated mice that were intraperitoneally injected with the probe **RO610** followed by saline only (no zymosan) showed a slight fluorescence enhancement, indicating that **RO610** was sensitive enough to detect native  $\text{ClO}^-$  levels in nude mice without external stimulation. The result established that **RO610** was a desirable imaging agent for visualizing endogenous  $\text{ClO}^-$  in vivo.

## Conclusions

In summary, a new rhodol dye **ROA** with an aldehyde group has been successfully developed, which exhibits high extinction coefficients, quantum yield, and good photostability. Based on the model platform, **RO610** was synthesized and it displayed a high sensitivity, selectivity and short response time for  $\text{ClO}^-$  over other related species. A549 cells and living mice imaging studies showed that **RO610** could be used as an effective fluorescent probe for detecting  $\text{ClO}^-$  in biological systems. Furthermore, **RO610** successfully achieved in vivo detection of endogenous  $\text{ClO}^-$  directly by using living mice without external stimulation. We believe the probe **RO610** can be regarded as a

worthwhile tool for investigating the roles of  $\text{ClO}^-$  in biological and pathological processes.

## Conflicts of interest

The authors have no conflicts of interest to declare.

## Acknowledgements

This work was supported by the National Natural Scientific Foundation of China (No. 21472148 and 21072158), Overseas Students Science and Technology Activities Project Merit Funding of Shaanxi Province (No. 20151190) and Academic Backbone of Northwest University Outstanding Youth Support Program.

## Notes and references

- (a) B.C. Dickinson and C.J. Chang, *Nat. Chem. Biol.*, 2011, **7**, 504-511. (b) T. Finkel and N.J. Holbrook, *Nature.*, 2000, **40**, 239-247. (c) D. Oushiki, H. Kojima and T. Terai, *J. Am. Chem. Soc.*, 2010, **132**, 2795-2801.
- (a) M.A. Shannon, P.W. Bohn and M. Elimelech, *Nature.*, 2008, **452**, 301-310. (b) X. Jin, Y. Jia and W. Chen, *Sens. Actuators B.*, 2016, **232**, 300-305.
- (a) Y.W. Yap, M. Whiteman and N.S. Cheung, *Cell. Signal.*, 2006, **19**, 219-228. (b) M. Whiteman, P. Rose and L.S. Jia, *Free Radic. Biol. Med.*, 2005, **38**, 1571-1584. (c) F.C. Fang, *Nat. Rev. Microbiol.*, 2004, **2**, 820-832.
- (a) A. Daugherty, J.L. Dunn and D.L. Rateri, *J. Clin. Invest.*, 1994, **94**, 437-444. (b) D.I. Pattison and M.J. Davies, *Biochemistry.*, 2006, **45**, 8152-8162. (c) V. Rudolph, R.P. Andrié and T.K. Rudolph, *Nat. Med.*, 2010, **16**, 470-474. (d) F.H. Greig, L. Hutchison and C.M. Spickett, *Clin. Sci.*, 2015, **128**, 579-592. (e) Y.D. Zheng, H.G. Lu, Z. Jiang, Y. Guan, J.L. Zou, X. Wang, R.Y. Cheng and H. Gao, *J. Mater. Chem. B.*, 2017, **5**, 6277-6281.
- (a) H.N. Kim, M.H. Lee and H.J. Kim, *Chem. Soc. Rev.*, 2008, **37**, 1465-1472. (b) J. Du, M. Hu, J. Fan and X.J. Peng, *Chem. Soc. Rev.*, 2012, **41**, 4511-4535. (c) X.Q. Chen, T.H. Pradhan and F. Wang, *Chem. Rev.*, 2012, **112**, 1910-1956. (d) F.A. Mauguère, P. Collins and Z.C. Kramer, *Chem. Lett.*, 2015, **6**, 4123-4128. (e) X.J. Cao, L.N. Chen, X. Zhang, J.T. Liu, M.Y. Chen, Q.R. Wu, J.Y. Miao and B.X. Zhao, *Anal. Chim. Acta*, 2016, **920**, 86-93. (f) H. Li, C. Wang, M. She, Y. Zhu, J. Zhang, Z. Yang, P. Liu, Y. Wang and J. Li, *Anal. Chim. Acta*, 2015, **900**, 97-102. (g) Q. Chen, C.M. Jia, Y.F. Zhang, W. Du, Y.L. Wang, Y. Huang, Q.Y. Yang and Q. Zhang, *J. Mater. Chem. B.*, 2017, **5**, 7736-7742.
- (a) J. Chan, S.C. Dodani and C.J. Chang, 2012, **4**, 973-984. (b) M. Beija, C.A.M. Afonso and J.M.G., *Chem. Soc. Rev.*, 2009, **38**, 2410-2433. (c) S. Liu, J. Zhao and K. Zhang, *Analyst.*, 2016, **141**, 2296-2302. (d) C.X. Chen, D. Zhao and J. Sun, *Analyst.*, 2016, **141**, 2581-2587. (e) L.J. Hou, J. Feng and Y.B. Wang, *Sens. Actuators B.*, 2017, **247**, 451-460. (f) C.G. Dai, X.L. Liu and X.J. Du, *ACS Sens.*, 2016, **1**, 888-895. (g) Z.H. Li, R. Liu and Z.L. Tan, *ACS Sens.*, 2017, **2**, 501-505.
- (a) L.G. Lee, G.M. Berry and C.H. Chen, *Cytometry*, 1989, **10**, 151-164. (b) J.E. Whitaker, R.P. Haugland and D. Ryan, *Anal. Biochem.*, 1992, **207**, 267-279 (c) T. Peng and D. Yang, *Org. Lett.*, 2010, **12**, 4932-4935.
- (a) B.C. Dickinson, C. Huynh and C.J. Chang, *J. Am. Chem. Soc.*, 2010, **132**, 5906-5915. (b) K. Kawai, N. Ieda and K.A. Aizawa, *J. Am. Chem. Soc.*, 2013, **135**, 12690-12696. (c) H.

## ARTICLE

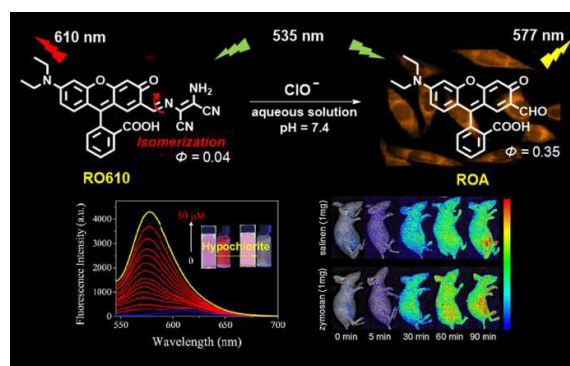
Journal Name

- Komatsu, Y. Shindo and K. Oka, *Angew. Chem. Int. Ed.*, 2014, **53**, 3993-3995. (d) X. Jiao, C. Liu and K. Huang, *Org. Biomol. Chem.*, 2015, **13**, 6647-6653. (e) L. Liang, L. Zhao and X. Zeng, *Rsc Adv.*, 2016, **6**, 85165-85172.
- 9 (a) J.S. Wu, W.M. Liu and J.C. Ge, *Chem. Soc. Rev.*, 2011, **40**, 3483-3495. (b) M. Emrulloğlu, M. Üçüncü and E. Karakuş, *Chem. Commun.*, 2013, **49**, 7836-7838. (c) S.I. Reja, V. Bhalla and A. Sharma, *Chem. Commun.*, 2014, **50**, 11911-11914. (d) Y. Wang, J.C. Xia and J.A. Han, *Talanta.*, 2016, **161**, 847-853. (e) P. Ghosh and P. Banerjee, *Anal. Chim. Acta.*, 2017, **965**, 111-122.
- 10 J.H. Chen, W.M. Liu and B.J. Zhou, *J. Org. Chem.*, 2013, **78**, 6121-6130.
- 11 G.W. Chen, F.L. Song and J.Y. Wang, *Chem. Commun.*, 2012, **48**, 2949-2951.
- 12 R. More and A.L. Capparelli, *J. Phys. Chem.*, 1980, **84**, 1870-1871.
- 13 S. Kenmoku, Y. Urano, H. Kojima, and T. Nagano, *J. Am. Chem. Soc.*, 2007, **129**, 7313-7318.

# A highly sensitive and rapidly responding fluorescent probe based on a rhodol fluorophore for imaging endogenous hypochlorite in living mice

Yanhui Zhang<sup>a</sup>, Lin Ma<sup>b</sup>, Chunchao Tang<sup>b</sup>, Shengnan Pan<sup>a</sup>, Donglei Shi<sup>a</sup>, Shaojing Wang<sup>a</sup>, Minyong Li<sup>b,\*</sup> and Yuan Guo<sup>a,\*</sup>

## Graphical abstract



A novel fluorescent probe **RO610** was applied for the in vivo detection of endogenous  $\text{ClO}^-$  using living mice.